Phenomenological Model for Unified Representation of Fundamental Particle Masses

L. Schächter[1] and J. Spencer[2]
[1] *Technion-Israel Institute of Technology, Haifa 32000, Israel and*
[2] *SLAC National Accelerator Laboratory, Menlo Park, CA 94025-7015, USA*
(Dated: July 21, 2014)

A geometric representation of the ($N = 279$) masses of quarks, leptons, hadrons and gauge bosons was introduced by employing a Riemann Sphere facilitating the interpretation of the N masses in terms of a single particle, the Masson, which might be in one of the N eigen-states. Geometrically, its mass is the radius of the Riemann Sphere. Dynamically, its derived mass is near the mass of the nucleon regardless of whether it is determined from all N particles or only the hadrons, the mesons or the baryons separately. Ignoring all the other properties of these particles, it is shown that the eigen-values, the polar representation (θ_ν) of the masses on the Sphere, satisfy the symmetry $\theta_\nu + \theta_{N+1-\nu} = \pi$ within less that 1% relative error. These pair correlations include such pairs as $\theta_\gamma + \theta_{top} \simeq \pi$ and $\theta_{gluon} + \theta_H \simeq \pi$ as well as pairing the weak gauge bosons with the three neutrinos. The eigen-values form 6 clusters that are reflective of a "Periodic" Chart of the Particles. A function was established whose zeros were a good approximation to the masses (θ_ν). A Regge analysis for missing masses was carried out and some uses for particle fusion reactions were considered including energy production. It was shown that there are very few particles with spin (J) larger than $1 + \theta^3$.

PACS No's. 02.30.Mv, 02.40.Ky, 11.30.-j, 12.,12.10.Kt, 12.90.+b

I. Introduction

Mass is a property of matter that we take for granted but, other than experimental data, little is known about its origins or composition. At the macroscopic level it was first taken by Newton to summarize all the irreducible properties of a body [1] and especially inertia or its resistance to motion. Further, because force per se was invisible while mass manifests itself in all observable bodies, it was mass that defined force for Newton and not the reverse. Later Einstein [2] postulated that the gravitational mass equaled the inertial mass that might include energy in various forms some of which appeared to have no ponderable mass whatsoever.

At the microscopic level, it is taken first as a parameter in a Hamiltonian and after renormalization the resultant value is taken to be the inertial mass of a particle [3]. We take these values as given [4,5]. At the low-energy end we find a degenerate pair of zero mass bosons (the photon and gluon) and the three neutrinos (electron, muon and tau) [6]. At the high-energy end are the gauge bosons $W^{\pm}$ and Z, the Higgs and the top quark.

Spanning from zero to more than 100GeV, we introduce a geometric representation allowing us to posit a generating particle - the Masson (pronounced as one does the Muon). Associated with it, there is a generating function whose zeros are the masses of the particles. These masses can be projected onto a 2D Riemann Sphere of radius equal to the mass of the Masson that is determined by imposing the equivalent of a minimum action criterion.

The only particle that we think we understand is the photon with zero mass. Ignoring other hypothetical low mass particles such as the axion or graviton [5], the photon must move at the speed of light because there is no rest frame to measure the mass explicitly based on $m_0/\sqrt{1-\beta^2}$.

Thus, while we know how to determine the extreme [5], in general, we do not know the fundamentals underlying the other values. However, we do know, according to Sommerfeld [7], that it is not associated with the charge alone. He pointed out that given a macroscopic charge of finite radius and mass, the energy associated with the two is different. His approach was simple: denoting by $E_{\rm EM}^{\rm (rest)}$ the electrostatic energy of the charged particle when at rest and subtracting this energy from the electric and magnetic energy when the particle is in motion $E_{\rm EM}^{\rm (motion)}$, it was shown that the difference does not equal the kinetic energy of the particle. Recently, the Standard Model was used to calculate the masses of 10 light hadrons as reported by Dürr et.al. [8]. Normalizing to the mass of the Ξ baryon, they found good agreement with the observed data.

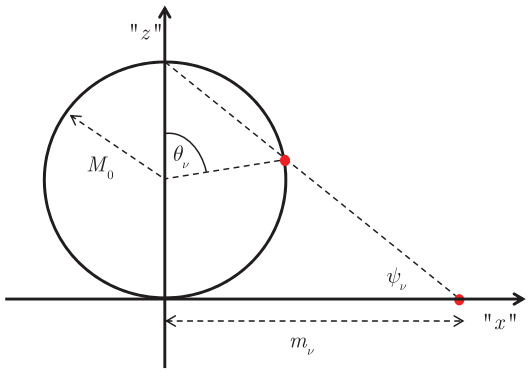

FIG. 1. The mass of a particle is marked on the axis (red-dot). Projection of the mass of the particle on the Riemann Sphere whose radius represents the mass of the Masson, is uniquely determined by the polar angle θ_ν .

We introduce a geometric (polar θ_ν) representation of the ($N = 279$) masses of the particles by employ-

Work supported by US Department of Energy under contract DE-AC02-76SF00515 and HEP.

ing a Riemann Sphere. This allows us to interpret the N masses in terms of a single particle, the Masson that may be in one of the N eigen-states and whose mass we take as the radius of the Riemann Sphere as shown in Figure 1. Ignoring the other properties of these particles, it is shown that the eigen-values satisfy the symmetry $\theta_\nu + \theta_{N+1-\nu} = \pi$ within less than 1% relative error. These eigen-values form at least 6 clusters that are representative of a "Periodic" Chart of the Particles.

We consider a form of Regge trajectory obtained from plotting the total spin J of some unflavored mesons and baryons separately as a function of their squared masses. This shows several linear correlations with some multiplets having five or more members but with conspicuous gaps or missing masses. Particle fusion possibilities are discussed that compare favorably to conventional sources of energy i.e. chemical and nuclear fusion and fission. Finally, some experiments that relate to inertial mass are discussed.

II. Riemann's Sphere

Because the range of the N masses span many orders of magnitude, we introduced a compact representation based on a Riemann Sphere as shown in Figure 1. The masses are organized in ascending order along the horizontal axis "x". The perpendicular axis is "z" and a flat-space Riemannian geometry is assumed. A circle of radius M_0 has its center at "x" $= 0$, "z" $= M_0$ and the intersection of the straight-line, connecting the top of the circle with "z" $= 0$, "x" $= m_\nu$ defines an angle θ_ν. Based on elementary trigonometric arguments one then finds

$$\theta_\nu = 2 \arctan\left(\frac{2M_0}{m_\nu}\right) . \qquad (1)$$

This transformation represents the projection of any one of the masses on the circle whose radius we attribute to the mass of the Masson. The latter is established next based on the experimental data and a minimal action criterion. To establish M_0, the vector θ_ν is organized in ascending order and we define the interval-spread of any two adjacent angles as

$$\mathcal{E}(M_0) = \frac{1}{\pi}\sqrt{\frac{1}{N+1}\sum_{\nu=0}^{N}(\theta_{\nu+1} - \theta_\nu)^2} . \qquad (2)$$

M_0 is the value that *minimizes* this functional; $\theta_{\nu=0} = 0$ and the $\theta_{\nu=N+1} = \pi$ represent the upper and lower limits of the masses in this polar representation. For the case of a *single* particle represented by an angle θ, there are two intervals: $\theta - 0$ and $\pi - \theta$ so the intervals spread is proportional to $\theta^2 + (\pi - \theta)^2$ and it has a minimum at $\theta = \pi/2$ implying for our simple case, the radius of the sphere is half the mass of the particle i.e. $M_0 = m/2$ or, equivalently, the particle's mass is twice the mass of the Masson: $m = 2M_0$.

Now we are in position to introduce the particles from the Table in Ref. [4]. The spread of their intervals in

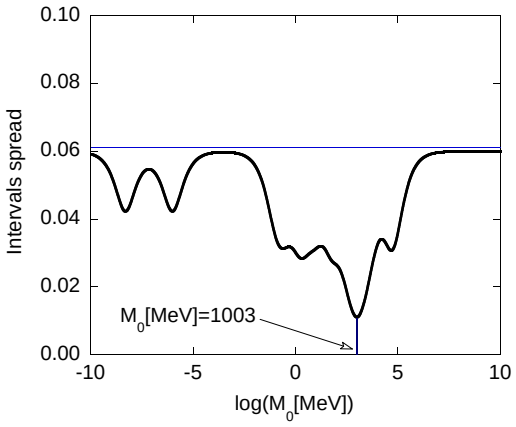

FIG. 2. Spread of intervals for N=279 fundamental particles as a function of M_0. The dominant minimum is calculated numerically and it occurs at M_0[MeV] $= 1003$.

Figure 2 shows clear resonant behavior. The absolute minimum represents the mass of the Masson occurring at 1003 MeV. For this value (M_0= 1003 MeV) the Riemann Sphere is illustrated in Figure 3. Two facts are evident – first, as anticipated, most of the particles are located in the $\theta \sim \pi/2$ region and, second, close to zero and π there are voids with no particles although these are not symmetrically disposed nor do they appear to be correlated in any obvious way but more on this later.

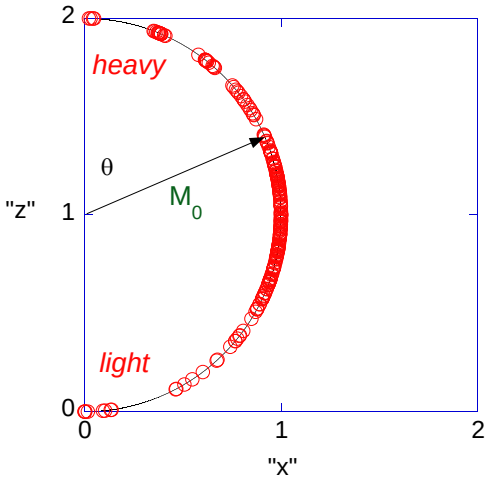

FIG. 3. Projection of the masses of all 279 particles where the mass of the Masson is determined from the requirement that the spread of the intervals in Figure 2 is minimal. Light particles ($\theta \sim \pi$) are the Axion, neutrinos and electron. The heavy ones ($\theta \sim 0$) the gauge-particles, Higgs and top quark.

III. Characteristics of the Polar Representation

With the polar representation established, we now investigate some features of the inertial masses based on this new representation. To begin, consider only the hadrons ($N = 261$). If we were to establish the Masson based on the hadrons alone, its mass would be only slightly reduced to $M_0^{(\mathrm{H})}$=962.2 MeV. Moreover, if we attribute a separate Masson to baryons ($N = 113$) and

to mesons ($N = 148$) the corresponding Massons would have masses of $M_0^{(\mathrm{B})}$= 1094 MeV and $M_0^{(\mathrm{M})}$=964 MeV. Also, the latter is close to both M_0 as well as to the stable nucleon mass N(940) and, curiously, there are more mesons than baryons even though their numbers of confined quarks(2) are fewer than for the baryons(3). In all three cases, the corresponding "intervals spread", as shown in Figure 2 for all of the particles, gave a *single* minimum.

Another perspective on the polar representation of the masses can be obtained by ordering θ_ν in ascending order and plotting them as a function of the index ν (quantum number) as the red squares in Figure 4. For comparison, the N zeros of the Legendre polynomial of order $N = 279$ are organized in ascending order and represented by the green squares $[P_N(\cos\zeta_\nu) = 0;\ \nu = 1, 2, ...N]$. While the latter is virtually linear, the former has a more complex structure with distinct "band-gaps" in the range $\nu < 0.2N$ and $\nu > 0.9N$.

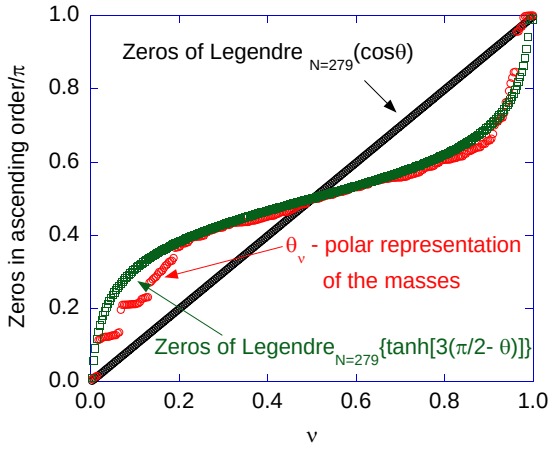

FIG. 4. Red squares represent the masses (θ_ν) in ascending order and the green squares the zeros of the Legendre function of order $N = 279$.

Two observations warrant attention: (i) if the absolute value of the argument of the Legendre polynomial is larger than unity the behavior is hyperbolic and the function has no zeros in this range. This explains the existence of the band-gaps. (ii) Having in mind that the argument of the Legendre polynomial ($\cos\theta$) varies between -1 and 1, we consider another function which is defined in this range (tanh) and we calculate the zeros of $P_N\left[\tanh\left(3.46\left(\pi/2-\theta_\nu^{(M)}\right)\right)\right] = 0$ which are represented by the black squares in Figure 4 where the superscript "M" indicates that this is a model. In the range $0.2 < \nu/N < 0.9$ these zeros approximate the polar representation of the masses (θ) with an accuracy of 0.07% being defined as $100 \times \left\langle [1-\theta_\nu^{(M)}/\theta_\nu]^2 \right\rangle_\nu$. What these results indicate is that the θ_ν may be regarded as the eigen-values of a characteristic polynomial of the Legendre type. Our approach was inspired by Liboff and Wang [9] in connection with their study of the prime numbers and the zeta function.

Having this representation in mind, an additional feature is revealed by examining the sum of the eigen-values. Let us assume that we know the Hamiltonian whose eigen-values are θ_ν^s wherein s is a free parameter to be determined. In many cases of interest, the measurable is given by a term of the form Trace (H) which in turn is proportional to $g(s) \equiv \sum_\nu \theta_\nu^s$. In reality we do not know this Hamiltonian however a rough idea as to its character may be assessed by assuming that $g(s)$ has a minimum. A simple calculation reveals that such a minimum exists for $s \simeq -79/150 = -0.5267$.

One of the main results of the present analysis relies on a property of the Legendre polynomials that the sum of *two zeros* of complementary order ($\nu+\nu' = N+1$) equals π, or explicitly $\zeta_\nu + \zeta_{N+1-\nu} = \pi$. We have examined to what extent this rule applies to the polar representation of masses (θ_ν) and we found $\theta_\nu + \theta_{N+1-\nu} = \pi\chi$ with $\chi = 0.958$ within 0.13% relative error defined as

$$\mathrm{Error}[\%] = 100\frac{1}{2N}\sum_{\nu=1}^{N}\left[\frac{\theta_\nu + \theta_{N+1-\nu} - \pi\chi}{\theta_\nu + \theta_{N+1-\nu}}\right]^2 . \quad (3)$$

The factor of 2 in Eq.(3) corrects the fact that each pair of masses is counted twice. According to the present spectrum of masses [4], this relation implies that the mass of the Higgs and that of the Axion (if observed) are related $\theta_{\mathrm{Axion}} + \theta_{\mathrm{Higgs}} \simeq \pi$ and the mass of the electrons neutrino is then related to that of the Z-gauge boson $\theta_{\nu_e} + \theta_Z \simeq \pi$ [5]. However, it should be emphasized that the present estimate of the error is dominated by the light particles $\theta \sim \pi$ and it is larger if the deviation is compared to the smallest angle between the two. In fact, due to uncertainty associated with the measurement of many of those masses and especially the neutrinos, comparing to the calculated deviation of χ from unity, we hypothesize that $\chi \equiv 1$ or explicitly

$$\theta_\nu + \theta_{N+1-\nu} = \pi \ . \quad (4)$$

Now we can use this symmetry to further quantify a Periodic Particle Chart. For this we plot in Figure 5 the normalized symmetry-pairs $(\theta_\nu + \theta_{N+1-\nu})/\pi$ as a function of the normalized masses (θ_ν/π).

Several important aspects are reflected in this plot: (i) the pairs determined in Eq.(4) form (at least) six clusters although a clearer picture will soon be revealed. (ii) The error or deviation from unity is dominated by light particles ($\theta \sim \pi$). When both particles have similar mass, the deviation is negligible $-$ see the right cluster. (iii) Further splitting is expected when including additional quantum numbers that produce a Riemann hypersphere. (iv) Subject to the condition $\chi \equiv 1$, the error defined above for hadrons is 0.47%, for baryons 0.07% and for mesons it is 0.63%.

Before we proceed, it is important to assess whether these small errors are the result of coincidence. For this let us postulate that the Masson has a fixed inertial mass

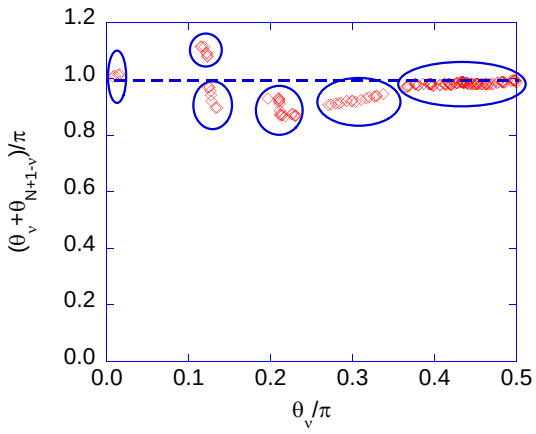

FIG. 5. The normalized symmetry-pairs, $(\theta_\nu + \theta_{N+1-\nu})/\pi$, as a function of the normalized geometric representation of the masses (θ_ν/π). These pairs form at least six clusters that resemble a "Periodic Table" for the fundamental particles.

of M_0=1003 MeV and between the two extremes, the photon and the top quark, the various (279) particles are randomly distributed. We represent the inertial masses in terms of a random variable $m_\nu\,[\mathrm{MeV}] = 10^{p_\nu}$ wherein p_ν is uniformly distributed $-8 \le p_\nu \le 5 + \log(1.26) = 5.104$. As in the case of the real particles, we employ the transformation in Eq. 1. It is tacitly assumed that the mass of the Masson is not dependent on the specific distribution. Once the θ_ν are established, the error is calculated based on Eq. 3. We determined this error 1000 times, each time for a different seed. The resulting error spans from 7% to less than 11%. Figure 6 shows the error as a function of the index of the seed $(1 \le n \le 1000)$. For comparison, in the case of all of the actual particles (279), its value is 0.225% indicating that the almost two orders of magnitude difference is not a result of coincidence.

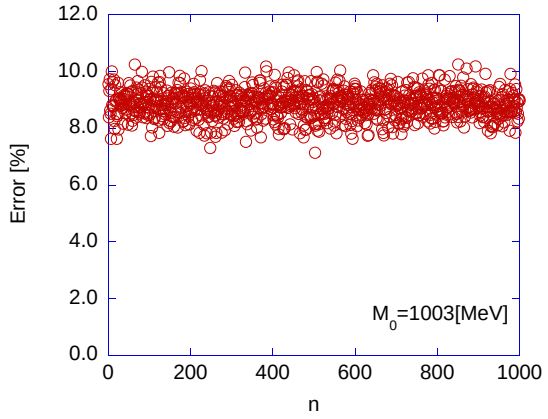

FIG. 6. The error associated with the polar representation of a random distribution of masses for 1000 different seeds. The value for the actual particles is 0.225%.

IV. Baryons and Mesons

Hadrons are the absolute majority (261) of the 279 fundamental particles we have considered and we have called them fundamental because they are composite being made of different numbers of quarks (and gluons or antiquarks) as opposed to those one might call elementary such as the electron. These particles can also be distinguished as bosons or fermions according to their individual spins. The elementary fermions include two classes - the quarks and leptons whereas the elementary bosons comprise the photon and gluons. As noted in the abstract, we have *not* included any antiparticles in our particle count. This was done because they bring nothing new to our analysis and because, as far as we know, there has never been a fermion discovered that did not lead to the discovery of its corresponding antiparticle with the possible exception of Majorana neutrinos.

This is one of the most important symmetries based on the unification of relativity and quantum theory by Dirac in 1928 [10] when studying the electron. Since that time it has been used for *all* spin one-half fermions including the proton and neutron with implications extending all the way to cosmological searches for anti-galaxies (*galaxies of anti-matter*) as well as why such objects have not been observed including several studies of how to observe or infer their prior existence.

We now take a closer look at the mesons (148) and baryons (113) separately and compare the two species. The Masson is assumed to have the mass as determined above $(M_0 = M_{Masson})$ and in the first row of Figure 7 we plot the polar intervals spread for both mesons and baryons - similar to the process that lead to Figure 2 except these spreads are only for mesons or baryons independently. A good approximation to the exact expression in Eq. (2), the (red) solid-line, is given by a simple Lorentzian (black) dashed-line corresponding to a band-pass model

$$\mathcal{E}_{\mathrm{model}}(M) = \mathcal{E}_{\max} + \frac{\mathcal{E}_{\min} - \mathcal{E}_{\max}}{\sqrt{1 + Q^2\left(\frac{M}{M_{\mathrm{Masson}}} - \frac{M_{\mathrm{Masson}}}{M}\right)^2}}$$

The spread of meson masses $(\Delta M = 5447\,[MeV])$ is more than twice the spread for the baryons $(\Delta M = 2506\,[MeV])$. Note that in these two cases, the intervals spread has a *single* resonance - contrary to the picture in Figure 2.

The central frames in Figure 7 show the normalized density of states (DoS) projected on the Riemann sphere when the arc is divided into 60 segments and a cubic spline is used to approximate the DoS function. Two comments may be made: (i) The resonance character of the DoS is clearly revealed and (ii) the voids and the structure in the DoS are more pronounced for the mesons. The bottom frames illustrate the complementary symmetry for each species. For the mesons we see 5 sub-groups but only 3 for the baryons but both particle types show a rough mirror symmetry about the central range $(\theta \simeq \pi/2)$.

V. Spin

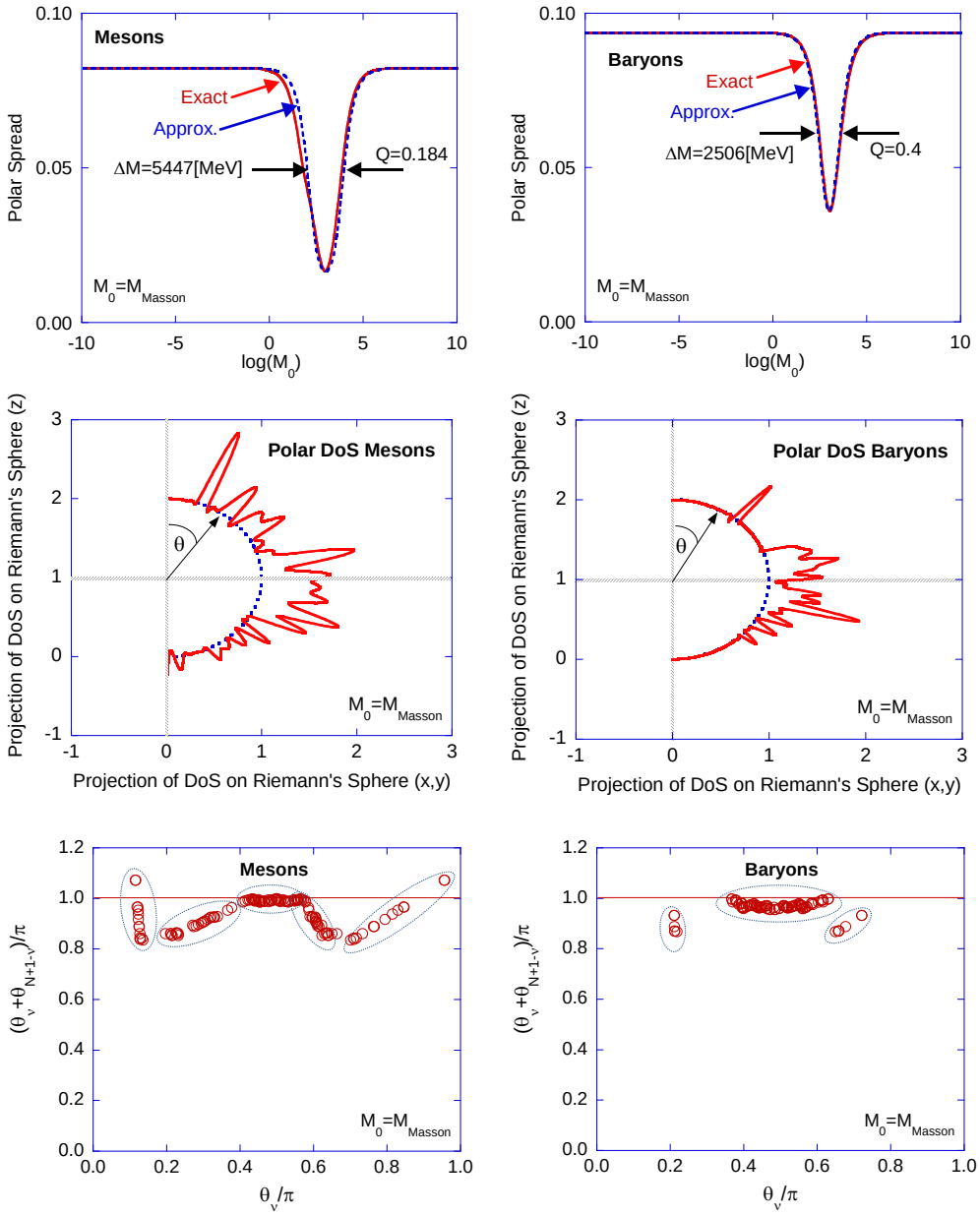

FIG. 7. Mesons (147) left-column and baryons (113) right-column are considered separately. The Masson is assumed to have the mass as determined above $M_0 = M_{Masson}$ and in the first row the polar intervals spread for both mesons and baryons are shown - similar to the process that lead to Figure 2 except the spread is only for mesons or baryons independently. A good approximation to the exact expression [Eq. 2], (red) solid-line, is given by a simple Lorentzian (black) dashed-line corresponding to a band-pass model. Central frames reveal the normalized density of states (DoS) projected on Riemanns sphere; the arc was divided into 60 segments and a cubic spline was used to approximate the DoS. Two comments are: (i) The resonance character of the DoS is clearly revealed and (ii) the voids in the DoS are more pronounced for the mesons. Bottom frames illustrate the complementary symmetry for the mesons and baryons. For the mesons we identify 5 sub-groups but only 3 for the baryons.

At this point we take one more step and introduce information about the total spin J. The four frames of Figure 8 reveal the polar representation of the masses as a function of the quantum numbers (ν) wherein the red circles represent the bosons (integer spins) and the blue crosses show the fermions (non-integer). The top-left frame reveals the overall picture whereas the other frames are magnifications of three ranges. Two facts are evident from the top-left frame: (i) there are significant voids at both low and high energy ends, (ii) bosons occupy most of the low-energy states ($\theta \sim \pi$) i.e. most of the lower-right frame.

At high energies (top-right frame) the voids become more distinct and there is no indication of a preferred

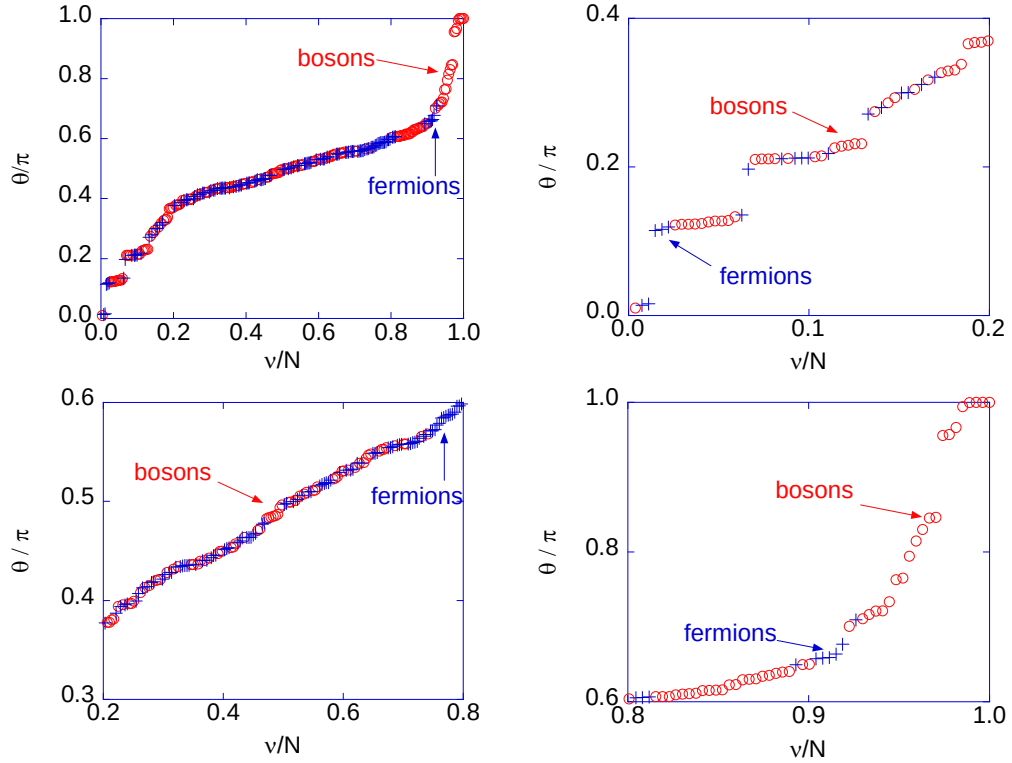

FIG. 8. Polar representation of the masses vs the quantum numbers for fermions(blue crosses) and bosons(red circles).

species (fermion or boson) in any one of the "energy-bands" with the exception of the last one. In the cental energy range ($0.2N < \nu < 0.8N$), bottom-left frame, θ is almost linear in ν and at the adopted resolution, there are, at most, two voids: (i) close to $\theta \sim \pi/2$ there is an interval that is fermions-free and (ii) at the top end there is a region which is bosons-free. With higher resolution, additional voids can be identified. Over the central range one can see a slight third order perturbation that gets considerably magnified at the wings (lower right frame). Finally, at the low-energy end (bottom-right frame), bosons dominate with four or five voids that are boson-free. Without more quantum numbers, we have no explanation for this "band-gap" structure other than greater sensitivity to the underlying quark masses.

Another observation refers to the distribution of fermions and bosons between spin-states. Figure 9 shows these distributions when each is normalized to unit area. Several comments can be made: (i) the peak distribution for the fermions is at the lowest state ($J = 1/2$) whereas the distribution of the bosons peaks at the first "excited state" ($J = 1$) and not the "ground state". (ii) The average quantum-number for bosons is close to $\langle J \rangle \sim 1$ while for fermions it is $\langle J \rangle \sim 1.5$. This contradicts distributions of single species of either bosons or fermions where in thermodynamic equilibrium, the highest likelihood is always the lowest or what we have called the "ground state" and this is also consistent with the Hamiltonian formulation. (iii) For both species, the spread is similar.

Figure 10 shows the spin J, θ and the symmetry

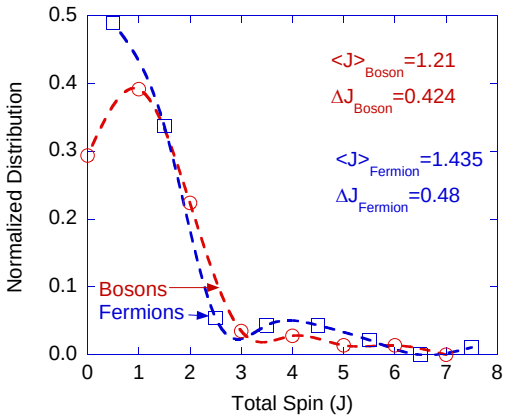

FIG. 9. Comparison of spin distributions: fermions(blue) and bosons(red). Fermions peak at one-half and bosons at one.

$\theta_\nu + \theta_{N+1-\nu}$ in one plot. Clearly, there are two major voids: the one on the left indicates no particles with a spin larger than $1+\theta^3$ and, on the right, that there are no lighter particles having $\theta > 0.6\pi$ with a spin larger than 2. We have no explanation for these two voids beyond our expectation that the highest spins should lie near the location of the highest density of states i.e. toward the middle.

VI. A Regge Approach

Initially, we simply plotted all the meson masses against other parameters and searched for linear trends.

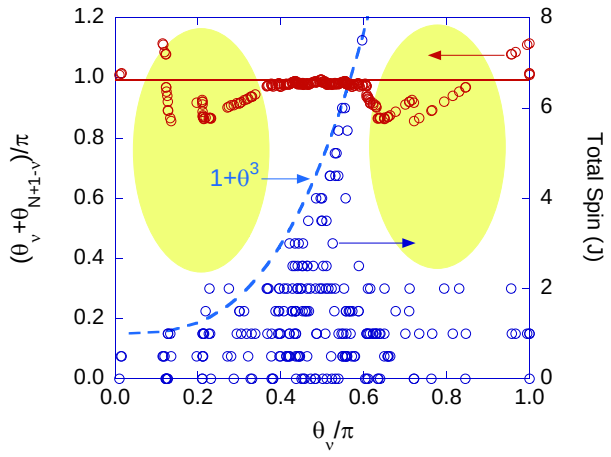

FIG. 10. The total spin J, θ and the symmetry $\theta_\nu + \theta_{N+1-\nu}$ are shown with two major voids (colored). The one on the left indicates that there are very few particles with a spin larger than $1 + \theta^3$ and, the one on the right, that there are no lighter particles having $\theta > 0.6\pi$ with a spin larger than 2. Rotating this figure shows an analog of the Periodic Table of the Elements based on the particle's total spin J.

Finding several quadratic curves among these we were led to the so-called Regge trajectories and their variants that provide methods to correlate and classify hadron states as well as to assign and predict their quantum numbers and masses. This makes expensive experiments much more efficient for discovering new results as shown in Figure 11 where the isoscalar $\eta(1405)$ is considered to be a candidate for the pseudoscalar $J^{PC} = 0^{-+}$ glueball and the isoscalar $\eta(1760)$ with its strong branching ratio to two gluons is called a gluonic meson. No attempt was made to incorporate the various quantum numbers for each particle into these trajectories or to make them the same for any trajectory in order to look for less obvious correlations e.g. others associated with quark molecules.

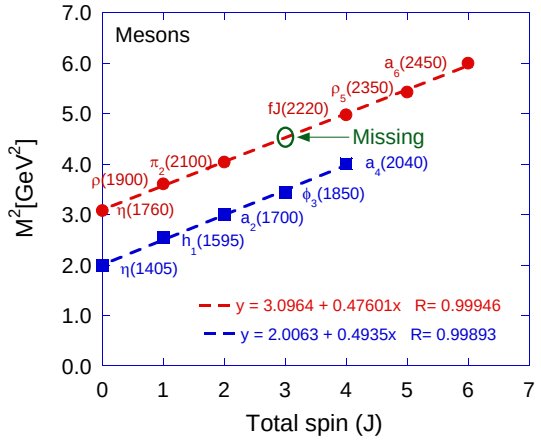

FIG. 11. Two parallel Regge trajectories for some heavier unflavored mesons characterized by their baseline η masses where the labels and the actual masses that were used are from Ref. 4. The missing mass at J=3 occurs near 2125 MeV.

Another plot for some unflavored lighter mass baryons is shown in Figure 12 where there are further missing masses. All of the nucleon states shown there are isospin doublets but the two trajectories distinguish two distinct classes. Because the two appear to share common spin and isospin characteristics one might assume that the N(1440) state is a radially excited n=2, 3 quark state of the nucleon N(940). Its prominent decay modes to the Nπ and $\Delta\pi$ have suggested a more complex 5 quark structure consisting of the 3 quark baryon and $q\bar{q}$ meson. We note that the two missing particles in these trajectories are expected to be P_{13} and H_{19} with masses near 1350 and 2410 MeV respectively as well as an additional higher spin state for the lower trajectory near 2200 MeV.

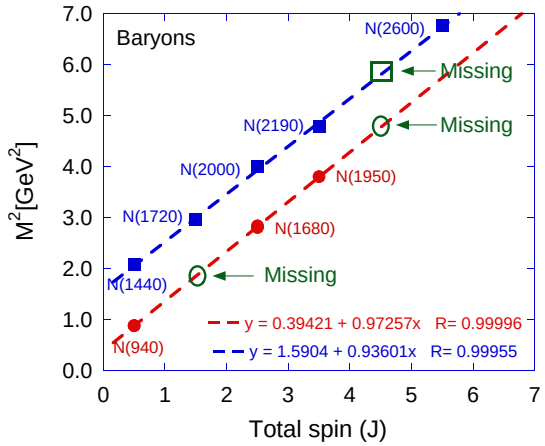

FIG. 12. Two parallel Regge trajectories for unflavored baryons characterized by their baseline P_{11} masses where the labels and the actual masses that were used are taken from Ref. 4. Missing masses occur at J=1.5 & 4.5 in the two trajectories near 1350, 2200 and 2410 MeV. Note that $P_{11} \equiv L_{2I2J}$.

VII. Particle Fusion Possibilities

When considering the structure of the mass eigenstates it is interesting to explore any energy opportunities they might provide as done for the atomic elements e.g. fusion reactions can be thought of as the dual of fission reactions in that to gain energy, fusion combines two light nuclei into one while fission splits one heavy nucleus into two. Because of the difference in binding energies per nucleon between the initial and final states of roughly 1 MeV, one expects to gain about 200 MeV per fission reaction in nuclei. Compared to a chemical reaction of only a few hundred eV per reaction one obtains a relative gain of the order 10^6 discounting any differences in the masses of the reactants (electrons).

For fusion, one expects a roughly order of magnitude lower energy gain per reaction than for fission but because fission reactions are much "dirtier" and the gain per kG of fuel is much better for fusion, it is preferred **if** an industrial-scale plant could be built. This is ironic considering the primary source of energy production in the universe is fusion but we only harvest it as solar power.

A major interest in heavy ion fusion lies in the hope of extending the periodic table well beyond its present range as well as extending nuclear models to much higher levels of atomic number and mass with important implications for states of very high angular momenta and large deformation. The range of ions and reaction energies of interest is also driven by the need for input into astrophysical calculations.

Lighter mass fusion reactions are well known from the (p,n), (d,t) and (d,He^3) reactions that release increasing amounts of energy per reaction. Such reactions are increasingly favorable up to Fe and Ni because the binding energies per nucleon are increasing up to this area.

Our reason for discussing fusion reactions is because they appear to be one of the better possibilities for the controlled production of energy using the fundamental particles and, more importantly, it seems to follow from the above discussion that the energy gain per unit mass of fuel could be much greater than for conventional fuels and methods thereby negating at least some of the obvious disadvantages.

As examples, consider the simplest, least exotic reactions: p + n $\rightarrow$ d + Q_n where $Q_n \approx$2.22 MeV and p + p $\rightarrow$ d + e^+ + ν_e + Q_p where $Q_p \approx$0.42 MeV whereas the d,t reaction yields 17.6 MeV. The e^+e^- annihilation gives $Q_{ee} \approx$1.02 MeV and the p^+p^- gives $Q_{pp} \approx$1.88 GeV. These appear nearly optimal in terms of their reduced energies per reaction ($\zeta \equiv \delta E/\delta M_r$) where ζ is a dimensionless figure-of-merit based on normalizing the output energy by the reduced mass M_r of the reactants. Said another way, the annihilation reaction that totally converts the mass of the reactants into free energy is ideal because it approaches perfect reaction efficiency and gives ζ=4 while a typical fission reaction gives only 0.004 and the pp fusion chain reaction (above) in the sun leading to He^4 yields 0.055. While these are not the best examples, they provide a proof of principle if not the practicality of such approaches because they are equivalent to nuclear fusion and fission processes at the microscopic level that reflect the dominance of the strong interaction of which the nuclear force is only a residual.

Some more interesting examples are those based on possible beam-dump experiments. This approach allows us to ignore the high incident energy overhead and simply consider the decay chain of one or more possible cascade reactions such as the $\Xi^o \rightarrow \Lambda^o + \gamma$ with $\Lambda^o \rightarrow$ p+π^- yielding nearly 380 MeV per reaction that we will take (arbitrarily) as a rough average over all possible outgoing reaction channels.

The design of the dump/target configurations for such possibilities presents some intriguing problems and opportunities. While practical questions such as the cost of both the power plant and the fuels are certainly relevant, they are beyond our interest here.

VIII. Other Experiments

Before concluding, additional comments on possible experiments will be made. A comprehensive review of neutrino oscillation experiments to determine neutrino characteristics such as their numbers and masses was given by Feldman et. al. [11]. Eddington's 1919 experiment [12], using the total solar eclipse of the Sun, confirmed Einstein's General Theory of Relativity that light "bends" in a strong gravitational field. One experiment we propose is to test the Equivalence Principle using neutrinos – the lightest inertial particles. As uncharged fermions their masses should be easier to understand than the other leptons that are considered to be pointlike based on all measurements of the electron to date. The problem is compounded when one considers their electromagnetic moments so it seems clear that neither leptons nor quarks are understood. Further, there is virtually no doubt that neutrinos do have mass because they form a triplet even though m_{ν_e} and certainly the axion may be too small to measure directly at this time.

Accepting that we cannot directly measure the mass of a neutrino, another way to study whether they are truly inertial in some sense or whether their mass results solely from their energies as with photons is to use a supernova or certain binary stars. Such systems could simultaneously provide photons for cross calibration and synchronization and another independent mass measurement if the neutrinos (and photons) pass close enough to a strong gravitational attractor along their paths to earth. We emphasize that we are also proposing a new Eddington type of experiment but for a possible photon mass e.g. by systematically varying the photons energy using lasers and satellites.

Finally, it is interesting to study and search for remnants of large annihilation events from anticomets or antiastroids or the missing masses in Fig's. 12 and 13 as well as various hypothetical particles each with their own unique problems of detectability.

IX. Conclusions

A geometric representation of the $N = 279$ **masses** of the elementary and lowest lying fundamental particles was introduced by employing a Riemann Sphere. It allowed us to interpret the N masses in terms of a single entity, the Masson, that might be in one of the N eigen-states. Geometrically, the mass of the Masson was the radius of the Riemann Sphere while its numerical value was closest to the mass of the nucleon regardless of whether M_0 was computed from all particles (279), the hadrons (261), or just the mesons (148) or baryons (113).

Ignoring the other properties of these particles, it was shown that the eigen-values, the polar representation (θ_ν), satisfy the symmetry $\theta_\nu + \theta_{N+1-\nu} = \pi$ within less than 1% relative error. One thousand samples consisting of 279 masses chosen randomly over the observed mass range gave much larger errors e.g. none were less than a factor of 30 larger. A function was established whose zeros were, to good approximation, the polar representation of the masses θ_ν. A rough assessment of the Hamiltonians's character was made by imposing that its trace $\sum_\nu \theta_\nu^s$ has a minimum for s=-0.523.

Among other results we found that bosons occupy most of the light mass states and there are virtually no fundamental particles with spin J larger than $1 + \theta^3$. Among hadrons we found that mesons form 5 clusters whereas baryons form 3 but both clusters have a similar structure being roughly symmetric about $\theta_\nu = \pi/2$. This suggests the "periodic-like" arrangement shown in Figure 10.

The new symmetry and its extension pairing bosons and fermions based on grouping all of the degenerate zero mass particles into one we will call the "photon" holds well for the gauge bosons and the lowest lying leptons and quarks until one has to pair hadrons because the quarks and leptons are fermions while the highest lying hadrons are bosons based on high lying, quark-antiquark mesons. The first breakdown occurs when a pion has to be used for the lowest member of a pair but there are more than 30 missing baryons according to this extended symmetry with some having low energies according to Figure 12.

We did not include antiparticles in our analysis because every fermion has a corresponding antifermion [10] so they added nothing new. Nevertheless, they are important for cosmology where the lack of any apparent antimatter in the universe is a concern when one expects anticomets and antigalaxies. Because the most disruptive body that might hit the earth is one made of antimatter this suggested some interesting experiments e.g. searches for the remnants of such an event. However, it must be noted that because the only stable hadron is a baryon one sees the weakness of using only classical concepts in an attempt to understand the microscopic particle world.

A Regge type analysis was carried out for mesons and baryons that suggested missing members for each type while providing different amounts of information on the missing masses quite apart from their masses and spins. Additional plots could be produced by filtering the data with differing constraints on the other quantum numbers. Similarly, the plot variables could be changed i.e. one could use other spin and isospin components to look for correlations between their results to search for the best experiments.

Particle fusion possibilities, including annihilation reactions between various leptons, baryons and their antiparticles, were suggested because these were the reactions with the best energy efficiencies and zetas (ζ). However, some very fundamental tests could also be performed in this realm if non rudimentary nuclei and their anti-nuclei could be produced - even with relatively few particles per beam but matrix beams [13] could be used to reduce space charge limitations for higher currents.

Acknowledgments

We acknowledge one of the great scientific achievements of the last 150 years on this anniversary of Mendeleyev's Periodic Table of the Elements. This was our inspiration and one reason we tried to confine ourselves to using only the masses. We especially wish to thank Stan Brodsky and Achim Weidemann for their valuable comments on the manuscript.

[1] Edwin Arthur Burtt, *The Metaphysical Foundations of Modern Physical Science*, (Routledge and Keegan Paul LTD, London, Revised Edition, 1932).

[2] Albert Einstein, "Elementary Derivation of the Equivalence of Mass and Energy," in *The Eleventh Josiah Willard Gibbs Lecture*, (Pittsburgh, 1934). Albert Einstein, "Ist die Trägheit eines Körpers von seinem Energiegehalt abhängig?," Ann. Der Physik **17,** (1905).

[3] We take as given that the equations of motion represent a set of coupled equations including all relevant variables with their couplings explicit e.g. the spins and isospins and whether we are solving the Lorentz equations, the Klein Gordon, the Dirac or the QCD Lagrangian, the mass of a particle or its reduced Compton wavelength always appears explicitly e.g. as a baseline potential.

[4] Rev. Part. Prop., Phys. Lett. B, Vol. **667/1** (1-1340) (2008). Also: Rev. Part. Phys., J. Phys. G, Vol. 37, 7A(1-1422) (2010). The exact Table used can be found at http://webee.technion.ac.il/people/schachter /AppendixMassesofFundamentalParticles.pdf

[5] We take the "rest mass" as simply "mass" – a relativistic invariant with neither "rest" nor the subscript "0" attached except for our hypothetical Masson M_0. The *observed* masses [4] are understood to be somewhat greater than the bare mass due to self interaction contributions. The Axion was included but not used and because we did not consider gravity, the graviton was not included. Neither of these have yet been observed.

[6] Because the error bars on the neutrino masses are large, we assume their masses are all much lighter than the electron's based on the standard model of cosmology.

[7] Sommerfeld A. , *Electrodynamics* in *Lectures on Theoretical Physics*, (Academic Press, New York, 1952), pp. 278.

[8] S. Dürr, Z. Fodor, J. Frison, C. Hoelbling, R. Hoffmann, S. D. Katz, S. Krieg, T. Kurth, L. Lellouch, T. Lippert, K. K. Szabo, and G. Vulvert, "Ab Initio Determination of Light Hadron Masses," Science, **322,** 1224 (2008).

[9] Richard L. Liboff and Michael Wong, "Quasi-Chaotic Property of Prime-Number Sequence", Int. J. Theo. Phys. **37,** 3109-3117 (1998).

[10] P. A. M. Dirac, "The Quantum Theory of the Electron", Proc. Roy. Soc. **A:** Math., Phys. & Eng. Sci. **117,** 610 (1928).

[11] G.J. Feldman,J. Hartnell, T. Kobayashi, "A Review of Long-baseline Neutrino Oscillation Experiments", arXiv.org, hep-ex, arXiv:1210.1778 (2013).

[12] F. W. Dyson, A. S. Eddington, and C. Davidson, Phil. Trans. Roy. Soc. Lon. A **220,** 291 (1920). For a good historical discussion see: Peter Coles, "Einstein, Eddington and the 1919 Eclipse," in *The Historical Development of Modern Cosmology* , (Proc. Int'l. School, Valencia, 2000).

[13] J.E. Spencer, "Study of Lattice Beams and Their Limitations', PAC2007 , Albuquerque NM.